Rayleigh-scattering-based measurement of 'trapped waves' in high-speed jets

Amy F. Fagan[1] and Khairul B.M.Q. Zaman[2]
NASA Glenn Research Center, Cleveland, OH, 44135, USA

Recently reported research by others identified a system of waves in the near-exit region of high-speed jets that are different from the well-known Kelvin-Helmholtz waves. In an experimental study, Rayleigh-scattering-based measurement of density fluctuations associated with these waves was used. Simultaneously, a microphone placed near the exit of the jet measured pressure fluctuations associated with the 'trapped waves'. The pressure fluctuations were observed as a series of peaks in the spectra. Measurements were acquired in high subsonic and under-expanded screeching supersonic flows from a 1-inch diameter convergent nozzle in a free jet facility. The Rayleigh measurement volume was translated throughout the flow field while the microphone was held fixed just outside the flow near the nozzle exit. Even though the signal-to-noise ratio for the Rayleigh data was poor, cross-correlation of density fluctuations with the microphone signal provided some insight into the propagation characteristics of the trapped waves as well as the screech component.

I. Nomenclature

c	=	ambient speed of sound
D	=	nozzle exit diameter
f	=	frequency
M_c	=	convective Mach number
M_j	=	jet Mach number
p_a	=	ambient pressure
p_0	=	plenum total pressure
PSD	=	power spectral density
r	=	radial distance from the jet centerline
SNR	=	signal-to-noise ratio
SPL	=	sound pressure level
St	=	Strouhal number
T_0	=	total temperature
U_c	=	convective velocity
U_j	=	jet exit velocity
x	=	axial distance from the nozzle exit plane
ϕ	=	phase
ρ	=	gas density
ρ_a	=	ambient gas density
ρ_j	=	jet exit gas density
ρ_{rms}	=	root mean square gas density fluctuations

[1] Senior Research Engineer, Optics & Photonics Branch, Communications & Intelligent Systems Division, Associate Fellow.
[2] Aerospace Engineer, Inlets & Nozzles Branch, Propulsion Division, Associate Fellow.

II. Introduction

Researchers have recently identified a system of instability waves in the potential core of high subsonic jets that are different from Kelvin-Helmholtz waves [1]. The phenomenon was detected in Large Eddy Simulations (LES) of a Mach 0.9 jet that was followed by analytical as well as some experimental verification. These 'trapped waves' were observed as a series of spectral peaks in the sound pressure level (SPL) spectra when measured near the edge of the jet. Perhaps the first experimental documentation of such pressure fluctuations can be found in an appendix of Ref. [2], where the 'spurious' spectral peaks were noted during a phased-array study of a subsonic round jet that were not understood. The LES data and analysis described in [1] show that both upstream- and downstream-propagating waves are supported, which result in the observed resonant tones. They observed that the shear layer acts as a duct confining the instability modes within the potential core of the jet. This is why the term 'trapped waves' was used to describe this phenomenon. The trapped waves are not detectable in the far-field, which is why they have been unnoticed for so long.

In the Fall of 2019, an experimental study was initiated at the NASA Glenn Research Center (GRC) to further study the phenomenon. Reference [3] documents SPL data acquired with a microphone placed in the near-exit region of high subsonic and low supersonic jets to measure the signature of the trapped waves for both round and rectangular nozzles. It was observed that these waves were not easily identified in the SPL spectra much beyond one jet diameter, mostly because the Kelvin-Helmholtz waves grow and dominate the downstream flow-field. A curious observation was that as screech ensued in the supersonic regime, the frequency of the audible screech tone appeared to lock onto one of the trapped wave frequencies. All of the experimental data used to characterize the trapped waves until now have been acquired via microphone instrumentation. Hotwire anemometry has been used extensively to study subsonic jets for a long time and, to the author's knowledge, has not shown evidence of the trapped wave phenomenon. This is likely due to the intrusive nature of such probes and the lack of their use in high-speed flows, due to their fragility. To overcome this challenge, the present study implements a non-intrusive laser-based Rayleigh scattering diagnostic to shed light on the characteristics of these trapped waves by way of measurement inside the jet potential core.

Molecular Rayleigh scattering is the result of elastic light scattering from gas molecules. If the gas composition is fixed, the total intensity of the Rayleigh scattered light is directly proportional to the gas density. A Rayleigh scattering diagnostic in the present experiment measures the scattered light from gas molecules in a small volume (~0.02 mm^3) using photomultiplier tube (PMT) detectors operated in the photon-counting mode to provide time-resolved density at a point in the flow field. This diagnostic was combined with simultaneous microphone measurements to provide unsteady gas density and sound pressure, respectively, in high-speed jets. Reference [4] discusses a similar type of Rayleigh scattering experiment (done in the same facility of the present study) where the density fluctuations were correlated with signal from a microphone placed in the far acoustic field (50D), with the objective of investigating jet noise sources. In the present experiment, the microphone was placed close to the jet's edge with the objective of investigating the newly discovered trapped wave phenomenon. The idea was that the cross-correlation between the two spatially-separated measurements (microphone at a fixed location in the near-exit region of the jet and Rayleigh probe varying within the jet flow field) will yield phase as well as amplitude information that would provide an insight into the characteristics of the trapped waves. A similar measurement technique shortly following the work of [4] implemented a two-point Rayleigh system to obtain the phase information from two spatially-separated density measurements. The data revealed the convective velocities of the coherent structures [5]. The measurements presented in [5] were all located outside of the potential core. In contrast, the current work presents density fluctuation data acquired within the jet potential core. The results illustrate that the Rayleigh diagnostic is capable of picking up the trapped wave signature in the density fluctuations. This diagnostic is a valuable tool for characterizing the trapped waves and validating the analytical models. A companion paper [6] discusses this phenomenon further in a microphone-based experimental study from the perspective of its relevance to jet noise applications and specifically addresses the relationship with screech tones.

III. Experiment

A. Facility and Instrumentation

Experiments were performed in an unheated small free jet facility (CW17) at NASA GRC. Compressed air passed through a plenum chamber before exhausting through the 1-inch diameter convergent nozzle into the ambient of the test chamber. Laser light scattered from air molecules in a small volume within the jet flow was used to measure time-resolved density. Since the molecular Rayleigh scattered signal was relatively low compared to that of

scattering from small particulates and nearby surfaces, precautions were taken to eliminate particulates in the jet air supply and stray light in the room. The unheated compressed air supplied to the jet was passed through micron filters to reduce the amount of dust, oil and water in the air. The total pressure (p_0) and total temperature (T_0) of the air flow was measured by a pressure transducer and thermocouple located in the plenum chamber, respectively. A pressure gauge provided the ambient pressure (p_a) in the facility. The sound pressure fluctuation spectra were measured by a ¼" microphone (B&K 4135) mounted near the jet exit while density fluctuations were measured simultaneously at a range of locations within the jet flow-field. The Rayleigh system was set up in two parts. The first part consisted of the laser and collection optics constructed around the jet facility. The Rayleigh scattered light was collected into an optical fiber and routed to another room where the signal detection took place. A photograph of the jet facility is shown in Fig. 1 and a detailed schematic of the measurement system is shown in Fig. 2. Measurements were acquired over a range of Mach numbers from subsonic to low supersonic regimes. The data are reported in terms of jet Mach number, M_j, which is defined as

$$M_j = \sqrt{\frac{2}{\gamma - 1}\left[\left(\frac{p_0}{p_a}\right)^{\frac{\gamma-1}{\gamma}} - 1\right]} \tag{1}$$

where γ is the ratio of specific heats for air. The microphone was held fixed at a position of (x/D, r/D) = (-0.25, 0.8), where the coordinate origin is located at the center of the nozzle exit and the axial (x) and radial (r) distances from the origin are nondimensionalized by the nozzle exit diameter (D). The microphone position in Fig. 1 is slightly different than was used for this experiment. The location is depicted more accurately in the schematic of Fig. 2 where it is in the same plane as the Rayleigh measurements and coming toward the jet exit from the side and at a slight angle. The Rayleigh measurement volume was varied within the jet flow field over a range of $0.2 \leq x/D \leq 12$ and $0 \leq r/D \leq 0.49$.

A 5 Watt 532 nm Nd:Vanadate continuous-wave laser with a 2.25 mm diameter output beam provided the incident light for the Rayleigh system. The laser was located in the test cell underneath the jet. The beam was routed via turning mirrors and focused by a 350 mm focal length lens (Lens 1, Fig. 2) to a 0.2 mm diameter beam at the probe volume. Rayleigh scattering is polarization dependent, so a half-wave plate was used to align the peak scattering plane with the collection optics. As shown in Figs. 1 and 2, the beam was aligned orthogonal to the jet axis and parallel to the ground. Scattered light was collected at a nominal angle of 90° to the incident light propagation direction. The collected scattered light was first collimated by an f/2.7 200 mm focal length achromat (Lens 2) and then focused by a 150 mm focal length achromat (Lens 3) onto the face of a 0.55 mm diameter multimode optical fiber. This optical arrangement provided a probe volume with a length of 0.7 mm and diameter of 0.2 mm. The laser, transmitting optics, and receiving optics were all mounted on the same axial-radial traversing mechanism (Fig. 1) so that the probe volume could be positioned anywhere in the flow-field.

The 20 m length optical fiber carried the scattered light from the facility location to the room where the detection optics, photon counting electronics, and data system were located. The light exiting the fiber was collimated by a 60 mm focal length f/2.4 lens (Lens 4) and focused by a 100 mm focal length lens (Lens 5) onto the sensor of the PMT. The PMT used for the density measurement was a Hamamatsu model R9110 detector tube with approximately 25% quantum efficiency at 532 nm, which was mounted in model PR1405SHCE housing by Products for Research. The PMT was operated in the photon-counting mode. The PMT was supplied with 1100 V and the photoelectron pulses were amplified with a gain of 5 before being sent to a Canberra model 2126 constant fraction discriminator, which output a TTL pulse for every photoelectron pulse exceeding the threshold discrimination level (-60 mV). The TTL pulses were counted by a National Instruments model 6602 counter-timer board. Typical photoelectron count rates were on the order of 10 MHz. A data acquisition system using LabVIEW™ software recorded the PMT counts and microphone signal records. The PMT and microphone channels were digitized for 30 s at a 40 kHz sampling rate. The microphone signals were low-pass filtered at 20 kHz. Spectral analysis was done over 0-20 kHz with 78 Hz bandwidth.

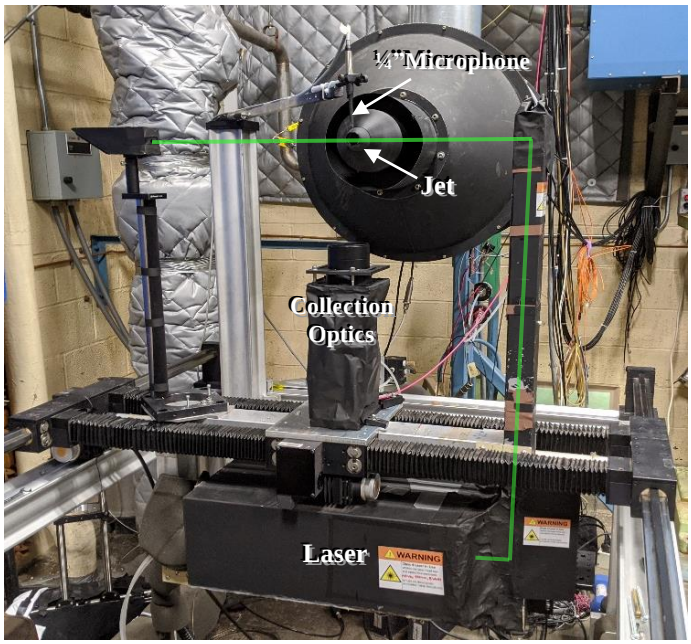

Figure 1. Photograph of jet facility and experimental arrangement.

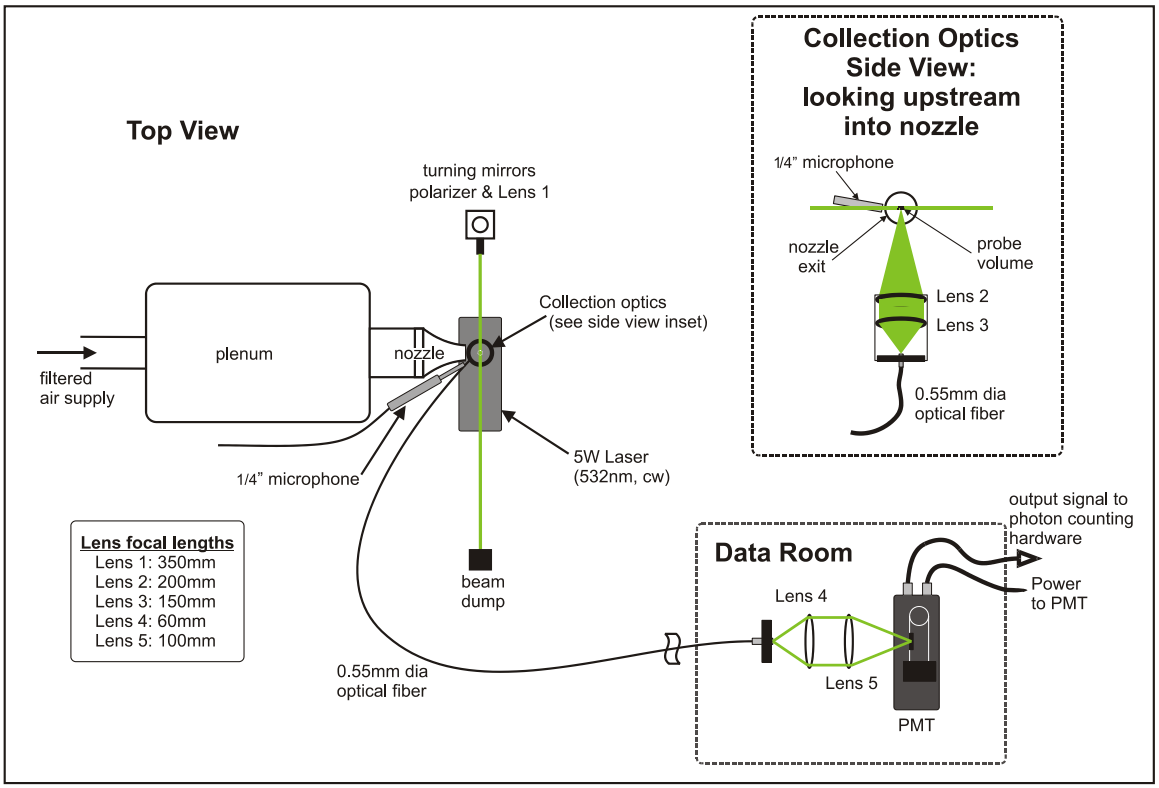

Figure 2. Schematic of setup for Rayleigh scattering based measurement.

B. Data Analysis

The PMT photoelectron counts in each data sample in the time-series accumulated over a time bin equal to the inverse of the sampling rate and the counts were directly proportional to the gas density. Calibration constants (slope and intercept) for this relationship were found using a linear least squares fit of the gas density as a function of PMT counts acquired over a range of jet Mach numbers (M_j = 0.18 to 1.0), while the Rayleigh probe volume was positioned within the jet potential core at x/D=0.2, r/D=0. The density for these calibration data points was calculated from isentropic flow relations using the measured total temperature (T_0) and pressure ratio (p_0/p_a). The photon counts in the subsequent data records were then converted to gas density using the established relation.

All Rayleigh measurements were performed within the bounds of the shear layer to avoid particle contamination; however, some particles were still encountered due to entrainment of dust from the ambient air, especially as the shear layer was approached. Particles passing through the measurement volume caused a very large spike in the photon counts. These spikes were filtered from the data and replaced with the mean value of the time-series. The percentage of replaced data points relative to the entire data record was quite low (<0.1%).

The SPL and density fluctuation spectra were calculated from the individual microphone and density data records as well as the cross-spectra of the two simultaneous measurements. For these calculations, the mean of each record was subtracted from the respective time-history record to provide zero-mean records. Because of the electronic shot noise in the Rayleigh signals, it was necessary to use relatively long data records along with a technique known as the Welch method of modified periodograms [7] to reduce the variance in the power spectral estimates. In this method, the data record was subdivided into smaller records, which were overlapped by 50%. The modified periodograms of each sub-record were calculated using a Hanning window. The individual periodograms were then averaged to obtain the estimate of the power spectrum and divided by the frequency bandwidth to obtain the power spectral density (PSD). The integral of the PSD is equivalent to the mean square fluctuations. The cross-PSD was calculated using this same Welch method. In the presented results, the length used for the sub-records was 512 and the resulting frequency bandwidth of the power spectra was 78 Hz.

A common numerical processing method used to eliminate noise from power spectra involves simply subtracting the noise floor from the spectra. Electronic shot noise was the primary source of noise in the photon count measurements. Shot noise is broadband noise that contributes equally over all frequencies and causes a constant offset in the spectrum. It is important to remove this noise component from the Rayleigh PSD because otherwise it is interpreted as additional rms density fluctuations, leading to high error in those measurements. In the case of the Rayleigh spectra, the noise floor was estimated from the average value of the last 1500 Hz of the spectrum where flow fluctuations were minimal. This value was subtracted from every point in the spectrum to eliminate the shot noise contribution from the PSD, as well as the mean square fluctuations that were calculated from the integral of the PSD. In theory, the shot noise is independent of the microphone signal and the cross-correlation process should remove it from the cross-PSD estimates; however, a residual level always remains. In [4] a no-flow spectrum was used to estimate this residual cross-spectrum noise floor. A no-flow spectrum was not acquired during this experiment and it was impossible to subsequently record this data due to closure of the laboratory for the COVID-19 pandemic. As an alternative, an estimate of the cross-spectral noise floor was made by cross-correlating the microphone signal with an unrelated low-speed, low-turbulence Rayleigh signal acquired during the calibration portion of this experiment. The fluctuations in these two signals should be completely uncorrelated and therefore should not show any significant correlation in the cross-PSD. The level of this spectrum should be indicative of the cross-PSD noise floor and the results of this analysis are presented in the next section.

IV. Results

Initially, microphone data were acquired with the same 1-inch diameter convergent nozzle mounted in two different free-jet facilities to verify that the trapped wave presence was not facility dependent. The first was a larger facility (larger plenum and supply lines, [3, 6]) than the one used in the present work. The second facility was the one detailed above and shown in Fig. 1. The microphone was placed near to the nozzle exit in both experiments and microphone signals were digitized at 100 kHz (50 kHz low pass filter) in the larger jet facility and at 50 kHz (25 KHz low pass filter) in the smaller jet facility. Although the latter data were acquired at a lower sampling rate, it was more than adequate to capture the range of frequencies of the trapped waves. The SPL spectra over the range 0-25 kHz are shown for the large and small jet facilities in Figs. 3 and 4, respectively. The jet Mach number was varied from about M_j = 0.7 up to M_j = 1.2 in each experiment. One can see that the same trapped wave spectral peaks were present in both facilities showing nearly identical behavior. As a screech tone became present at supersonic conditions, it appears that it locked onto one of the trapped wave frequencies. This observation was explored in

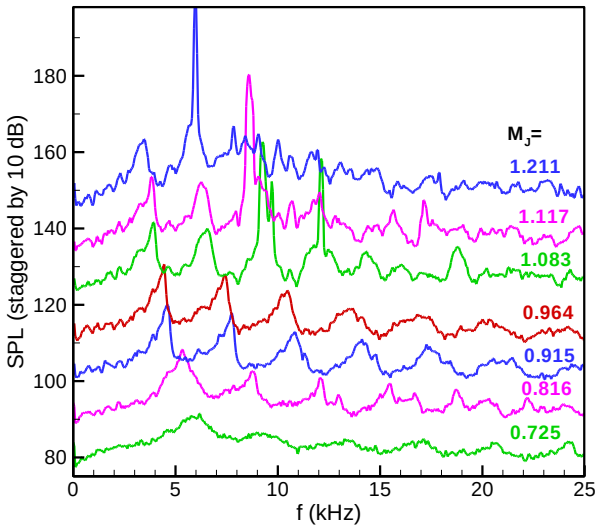

Figure 3. SPL spectra for the 1-inch convergent nozzle mounted on a large jet rig at varying M_j showing the trapped waves, and the screech component locking onto one of the trapped wave frequencies.

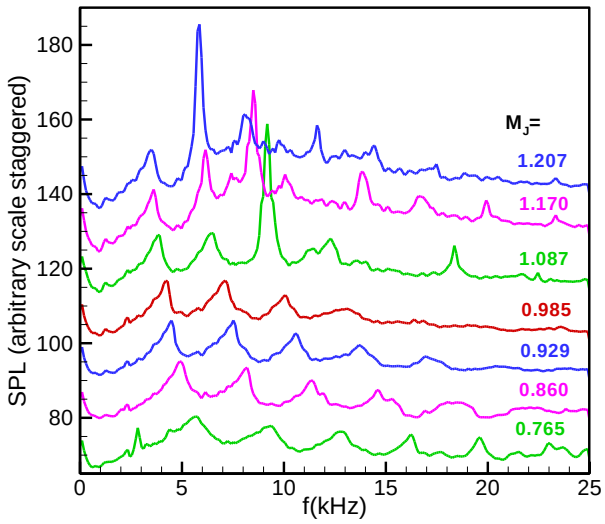

Figure 4. SPL spectra for the 1-inch convergent nozzle mounted on the current smaller jet rig at varying M_j showing the same behavior as observed in the large jet rig (Fig. 3).

more detail in [6]. For the remainder of the paper, all data presented were taken in the smaller jet facility described in Section III.

The Rayleigh technique was not as sensitive as the microphone measurements for detecting the relatively weak pressure fluctuations associated with the trapped waves. The signal-to-noise ratio (SNR) for a microphone measurement is typically greater than 10^6, whereas the SNR for the Rayleigh measurements presented here was only about 20. Using the higher sensitivity microphone to study the trapped waves from inside the flow field was not an option for the obvious reason of gross intrusiveness. Since the Rayleigh SNR is relatively low, it was important to confirm the ability of the technique to measure the jet density fluctuations. To this end, data were acquired at several downstream locations in a M_j = 0.97 jet where we expected to detect the jet 'preferred mode' waves (Kelvin-Helmholtz waves). The characteristics of these waves are well-known; a broadband fluctuation peak centered at frequency f is expected in the density fluctuation spectrum corresponding to a Strouhal number ($St=fD/U_j$), in the range of 0.3-0.5, the value of St decreasing with increasing x/D [8]. Figures 5(a) and 5(b) show the PSD curves of the Rayleigh density measurements at x/D= 2 and 3 (shear layer) and x/D= 4 and 6 (centerline), exhibiting the broadband peak at the expected range of St. This gave confidence that the Rayleigh measurement system accurately captures the density fluctuations in high subsonic jet flows and may be capable of detecting the trapped wave pressure fluctuations.

Simultaneous microphone and Rayleigh measurements were performed over a range of separation distances by holding the microphone fixed at the reference location (x/D=-0.25, r/D=0.8) while the Rayleigh measurement volume was translated axially and radially in the jet flow. For the M_j = 0.97 flow, measurements were acquired axially along the jet centerline and radially at two axial measurement stations. The normalized mean density and root mean square (rms) density fluctuations evaluated from the Rayleigh data are plotted for these axial and radial scans in Figs. 6(a) and 6(b), respectively. The data in Fig. 6(a) agree overall with data presented for a similar flow condition (M_j = 0.95) in Fig. 5 of Ref. [4]. Note that the mean density drops by about 10% before taking a sharp drop off at the end of the potential core (x/D=6). This is unlike mean velocity, which typically remains constant within the length of the potential core. The rms density fluctuations are also in general agreement with these previous measurements where the fluctuations increase sharply at the end of the potential core to a peak value of just over 20% at x/D=8 followed by a sharp decrease. The radial profile values in Fig. 6(b) follow expected trends as well. The mean values are nearly constant across the jet width until they fall off sharply at the shear layer. The rms values are about 4-5% in the jet core and climb rapidly as the shear layer is approached. Measurements through the full shear layer were not possible in this experiment due to particle entrainment. Also, the length of the measurement

volume in the direction orthogonal to the shear layer was about 0.7mm which was too large to resolve the shear layer accurately since the shear layer thickness was on the order of 1-3mm at these locations. However, the size of the measurement volume was sufficient for studying the trapped waves, which was the primary objective of this study. The data presented thus far prove that the Rayleigh technique is capable of measuring density fluctuations in high subsonic jet flows and is a promising technique for detecting and characterizing the trapped waves.

The PSD curves for Rayleigh data acquired at a few different locations in the M_j = 0.97 jet along with the corresponding microphone SPL spectra and cross-PSD are shown in Figs. 7(a)-7(c). The signature of the trapped waves is clear in the microphone spectra with the first three spectral peaks denoted with vertical dashed lines. However, the evidence is not obvious in the Rayleigh PSD at any locations in the jet. Thus, spectra of the Rayleigh signal alone did not reveal the trapped wave peaks, obviously due to high noise in the Rayleigh signal. However, the cross-PSD between the Rayleigh and microphone signals do show the correlation peaks, although weak, at the same

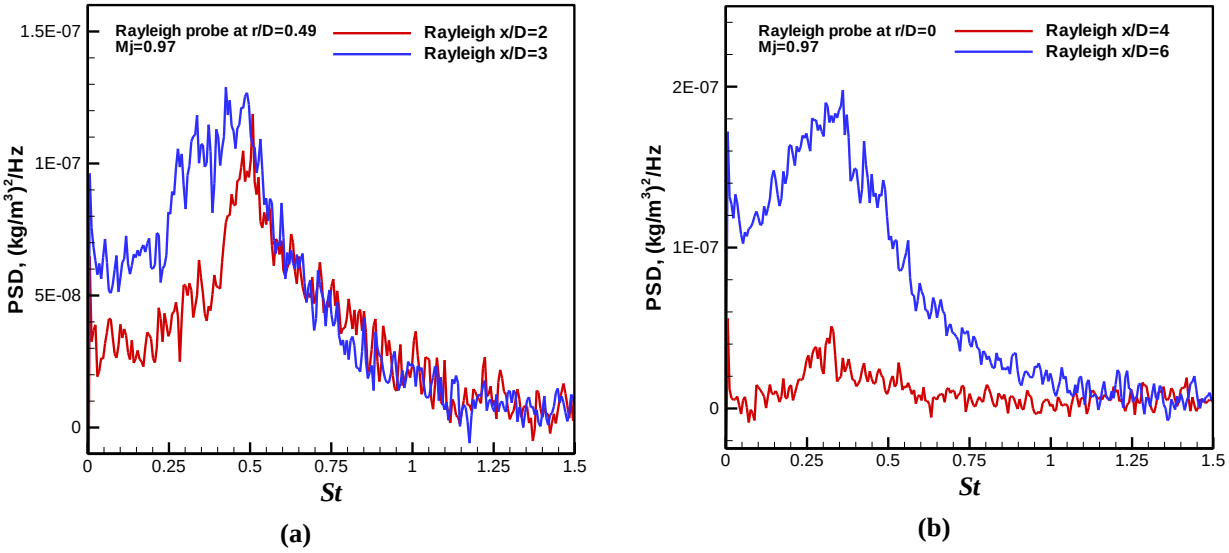

Figure 5. Rayleigh density fluctuation PSD in an M_j = 0.97 jet showing evidence of expected 'preferred mode' coherent structures (Kelvin-Helmholtz waves). Rayleigh probe location: (a) in the jet shear layer (r/D=0.49) at x/D = 2 and 3, and (b) on the jet centerline (r/D=0) at x/D = 4 and 6.

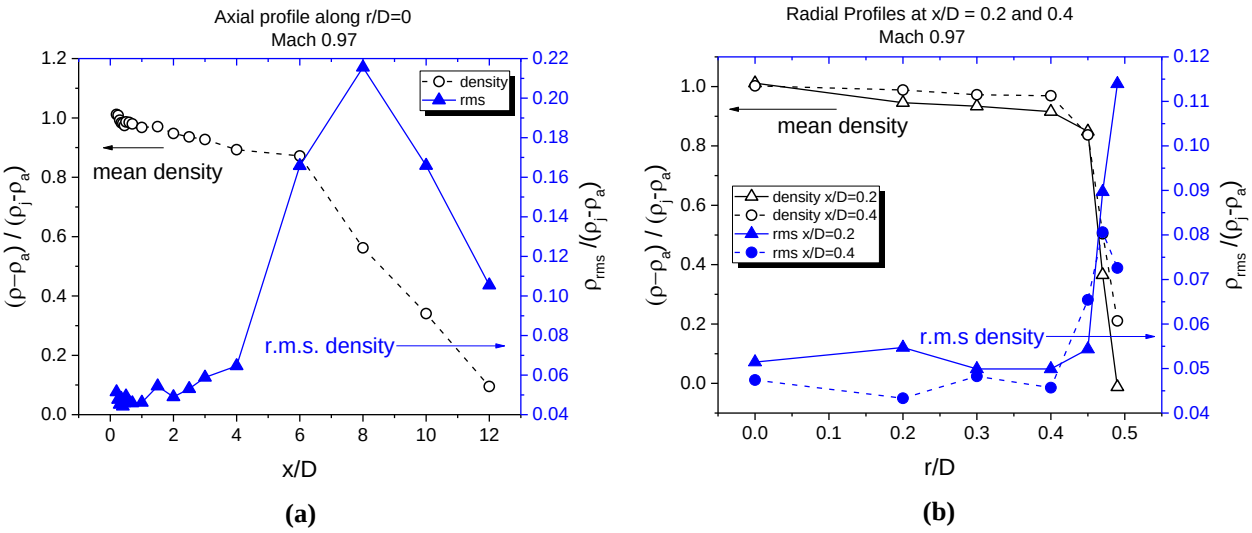

Figure 6(a). Mean and rms Rayleigh density profiles at M_j = 0.97: (a) centerline profiles (r/D=0), (b) radial profiles at axial stations of x/D = 0.2 and 0.4

three frequencies. The *x/D*=1.5 location in Fig. 7(c) has the largest amplitude cross-PSD peak at the first trapped wave frequency for this Mach number flow. The other two data sets (Figs. 7(a) and 7(b)) closer to the nozzle exit exhibit typical relative amplitudes observed in the cross-PSD signals for this flow.

As a means of estimating the noise floor for the cross-PSD measurements, the microphone signal at M_j = 0.97 was cross-correlated with an unrelated, low-turbulence Rayleigh data record from a different much lower speed (M_j = 0.18) flow acquired at a different time. These measurements should be completely uncorrelated and therefore represent the lower bound of the cross-PSD measurements. This correlation is represented by the green dashed correlation curve in Fig. 7(d); the upper bound of this correlation is taken as the noise floor and indicated by the horizontal cyan dashed line. The cross-PSD curves for the *x/D*=0.4 and 1.5 locations are plotted again in Fig. 7(d) for comparison with the noise floor. The first trapped wave spectral peak just barely exceeds the noise floor while the second and third trapped wave peaks are at or below it. The amplitude of the cross-PSD magnitude at the first three trapped wave frequencies of 4300 Hz, 7300 Hz, and 10200 Hz are plotted as a function of *x/D* and *r/D* in Figs. 8(a) and 8(b), respectively. The flat, low amplitude nature of the plots for the second and third trapped wave peaks gives further evidence that the fluctuations at these frequencies are below the noise floor of the current measurements. However, the first trapped wave spectral peak, which is shown to exceed the noise floor, exhibits reasonable trends radially and axially. In Fig. 8(a), the cross-PSD amplitude at *f*=4300 Hz increases axially along the centerline until the end of the potential core, then decreases steadily until it reaches the noise floor level (~2E-8) at *x/D*=12. In Fig. 8(b), the 4300 Hz cross-PSD peak at *x/D*=0.2 increases radially outward from the centerline until it peaks at *r/D*=0.3 after which it steadily decreases until it reaches the noise floor level at *r/D*=0.45. At *x/D*=0.4 the 4300 Hz peak amplitude is nearly constant until it reaches *r/D*=0.3 and starts to steadily decrease until it reaches the noise floor at *r/D*=0.45. These profiles for the 4300 Hz trapped wave do not exhibit any 'nodes' in the radial direction and thus suggest that the mode shape might be axisymmetric.

In summary, the data presented in Figs. 7 and 8 demonstrate evidence of the trapped wave pressure fluctuations via Rayleigh measurements inside the jet potential core, however the pressure waves are weak and do not exhibit a strong correlation at the higher frequencies given the low SNR of the existing Rayleigh system. Plans to improve the SNR in future measurements include implementing a photo sensor module that has a higher quantum efficiency and lower noise characteristics than the model used in this experiment. Additional ways to increase the signal strength are by using a higher power laser and directly coupling the signal to the PMT sensor instead of using fiber coupling. Taking a much longer time record should also reduce the variance in the power spectral calculations.

Data were also acquired in the under-expanded supersonic regime at M_j = 1.15. This was partly motivated by the fact that the screech component appears as if an extension of the trapped waves in the supersonic regime [6]. Again, the Rayleigh measurement volume was translated through a range of axial and radial locations while the microphone was held fixed at the reference location near the jet exit. The PSD of the microphone and Rayleigh density fluctuations are shown in Fig. 9(a) along with the corresponding cross-PSD at a Rayleigh measurement location of *x/D*=0.4 and *r/D*=0. This flow contains a screech component at a frequency of 8900 Hz as evidenced by the strong, narrowband peak in the spectra in Fig. 9. The strong peak at 8900 Hz in the Rayleigh PSD demonstrates that the Rayleigh diagnostic is sensitive enough to detect the stronger screech pressure waves in the density fluctuations. As stated already, the microphone SPL spectrum shows that the trapped waves persist into the supersonic regime, and in this case, the third trapped wave spectral peak appears to amplify and turn into screech. A similar exercise to estimate the noise floor of the cross-PSD was performed where the screech-containing microphone signal was cross-correlated with a completely uncorrelated, low-turbulence Rayleigh signal acquired in a M_j = 0.18 flow at a different time. This noise floor spectra is shown as the green dashed correlation curve in Fig. 9(b) along with the cross-PSD from Fig. 9(a). The average noise floor is about 5E-8 (arbitrary units) as indicated by the horizontal cyan dashed line. The trapped wave and screech spectral peak frequencies are indicated by the vertical dashed lines. The first trapped wave cross-PSD peak exceeds the noise floor and the screech peak is about two orders of magnitude above the noise floor; however, the other spectral peaks are at or below the noise floor.

Figure 9(c) shows the cross-PSD together with corresponding phase angle in radians. The phase information from the cross-spectra of two spatially-separated measurement locations can be used to calculate the phase velocity of the flow structures. The magnitude and phase of the cross-PSD at the screech frequency were tracked as a function of axial and radial location in the jet. Figures 10(a) and 10(b) document the cross-PSD and Rayleigh PSD amplitudes at *f*=8900Hz as a function of *x/D* along the centerline (*r/D*=0) and near the shear layer (*r/D*=0.4), respectively. The Rayleigh and cross-PSD amplitudes generally follow the same trend, further verifying that the SNR of the Rayleigh measurement is sufficient to detect the density fluctuations associated with the screech tone. The amplitudes along the centerline are found stronger than the amplitudes along the shear layer. In [9], noise sources in high-speed jets were investigated via correlations between flow density and far-field acoustic pressures where the peak correlation amplitudes as a function of axial and radial distance were presented for high subsonic

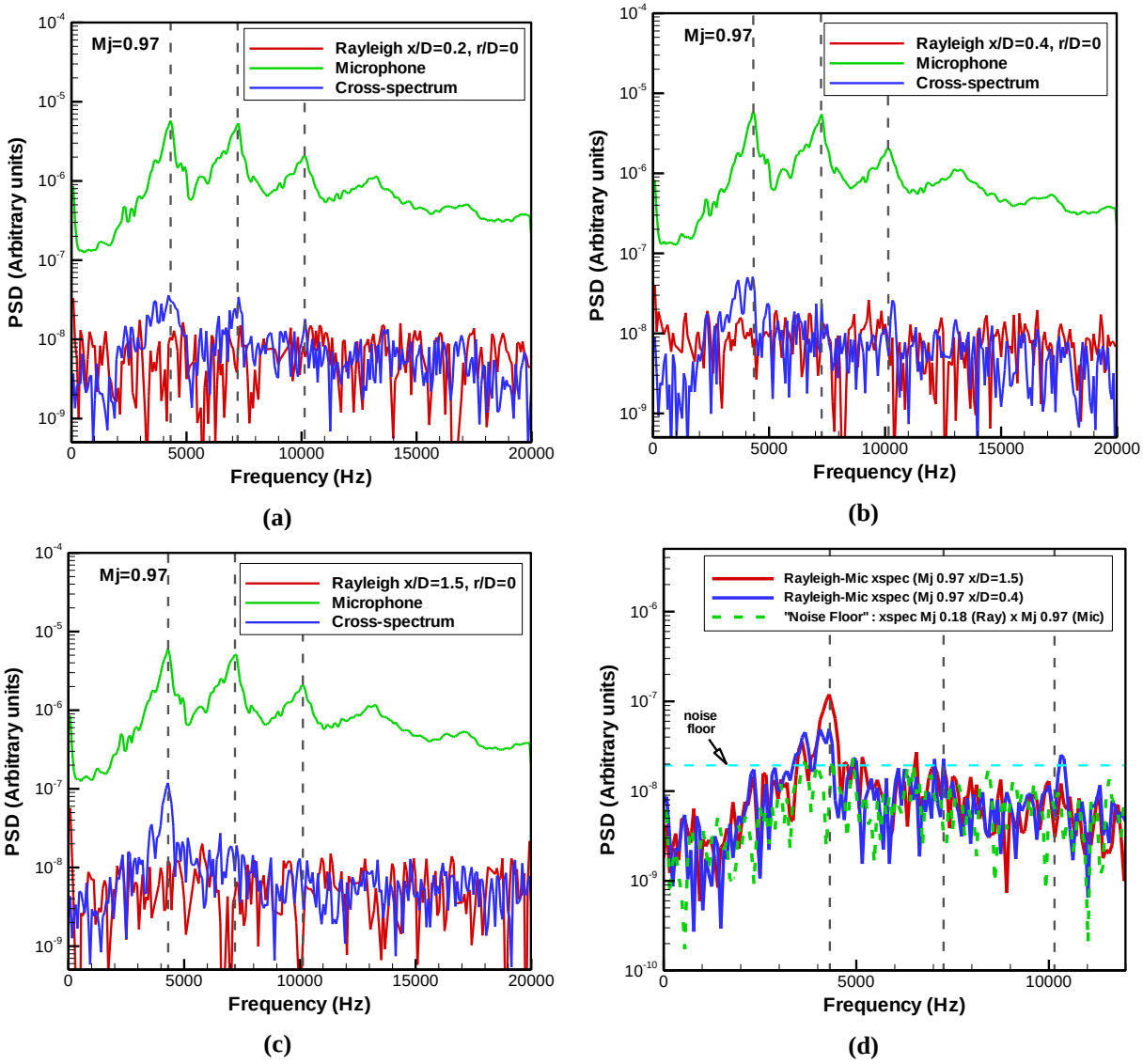

Figure 7. Rayleigh and microphone PSD curves and the corresponding cross-spectrum for M_j = 0.97 with the microphone at *x/D*=-0.25 and *r/D*=0.8 and the Rayleigh probe on the centerline at axial stations of (a) *x/D*=0.2, (b) *x/D*=0.4, and (c) *x/D*=1.5; (d) Cross-spectra noise floor estimation via correlation with unrelated Rayleigh signal at M_j = 0.18.

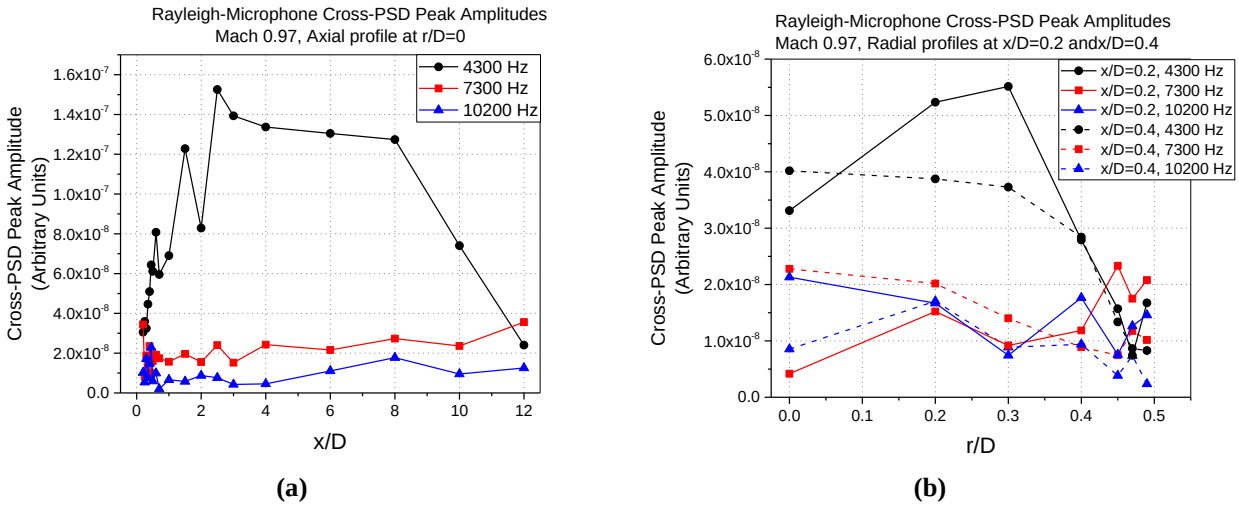

(a) **(b)**

Figure 8. Cross-PSD peak amplitude for the first three trapped wave frequencies at M_j = 0.97 as a function of (a) *x/D* along the centerline (*r/D*=0), and (b) *r/D* at axial stations of *x/D*=0.2 and 0.4.

and supersonic regimes. In this work, it was also found that the correlation peak amplitudes were stronger along the centerline than along the shear layer. Similarly, in Fig. 10(c) the cross-PSD and Rayleigh PSD amplitudes at f=8900 Hz are plotted as a function of *r/D* for an axial station of *x/D*=0.2. Figure 10(d) shows the cross-PSD phase, ϕ, as a function of *x/D* for the centerline and shear layer axial scans. The solid lines are the resulting linear least squares fit to the data; the slopes of the two data sets are nearly equal and indicate downstream propagating waves. (That it is downstream propagating was verified by introducing artificial delays in a signal and checking the slope). The convective Mach number, M_c, was calculated from the average slope ($\Delta\phi/\Delta x$=6.18=1.97π). From the relationship,

$$M_c = \frac{U_c}{c} = \frac{2\pi f}{c\,\frac{\Delta\phi}{\Delta x}} \tag{2}$$

where U_c is the convective velocity, f is the screech frequency, and c is the ambient speed of sound, the average convective Mach number was found to be M_c=0.67. A similar analysis of phase was performed using a laser light scattering technique to measure refractive index changes associated with density fluctuations of organized turbulent structures in the jet shear layer in [10] where the average M_c was measured as 0.7 for an M_j = 1.19 flow. Points shown in red in Fig. 10(d) are outliers, especially in the shear layer measurement, that were ignored in the fitting of the data. It is unclear if the outliers were due to 'noisy' measurements, or due to other components of the feedback loop involved in the screech phenomenon. Further exploration is planned with a finer resolution measurement grid and improved SNR to better track the phase of the propagating waves. Also, with improvement of the SNR, a more detailed study of the trapped waves and their propagation characteristics will hopefully provide further insight.

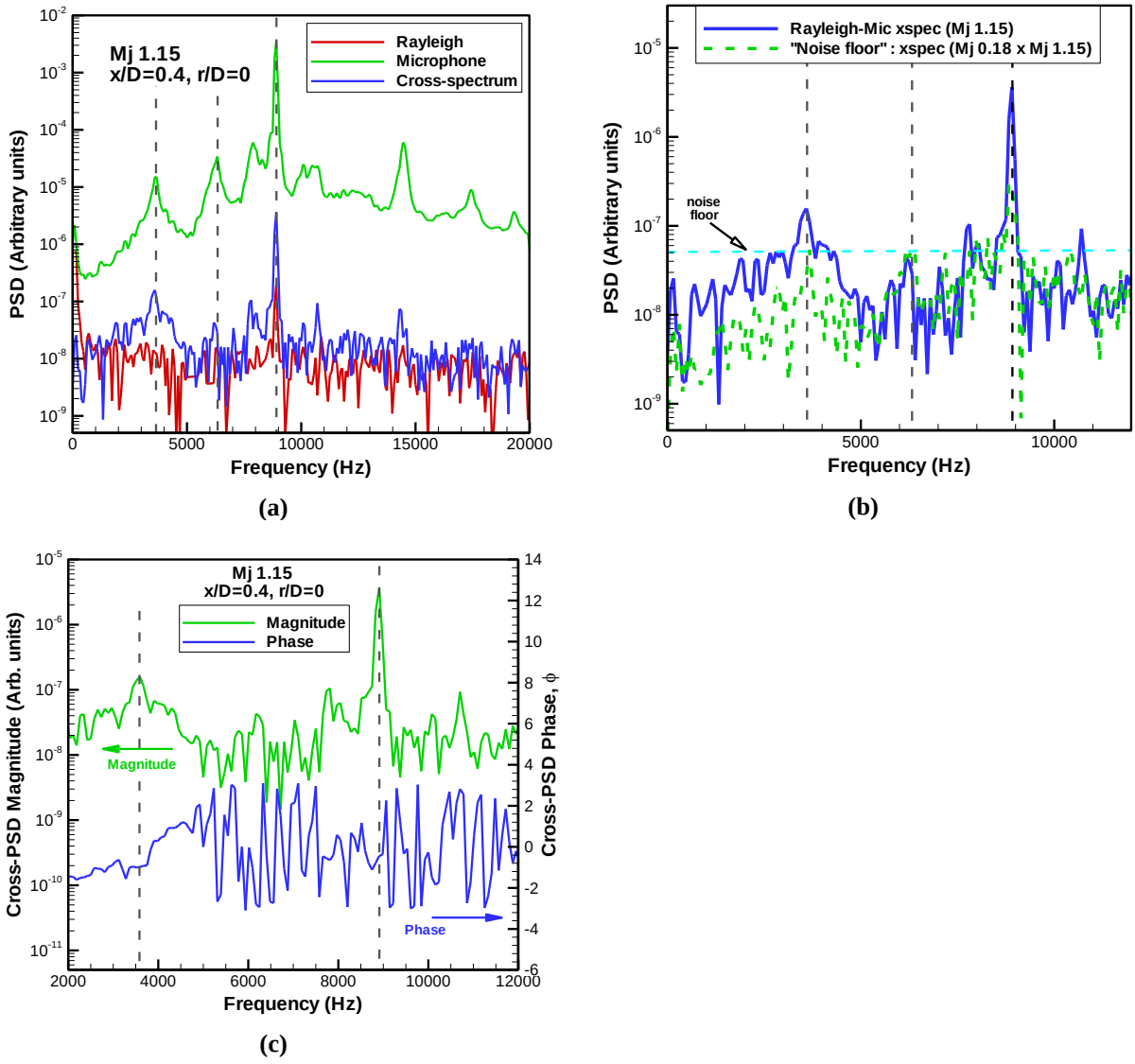

Figure 9. Rayleigh and microphone spectra for M_j = 1.15 with the Rayleigh probe at x/D=0.4, r/D=0 and the microphone at x/D=-0.25, r/D=0.8: (a) magnitude of the Rayleigh and microphone PSDs and their cross-PSD, (b) cross-spectra noise floor estimation via correlation with unrelated Rayleigh signal at M_j = 0.18, and (c) cross-PSD phase ϕ in radians.

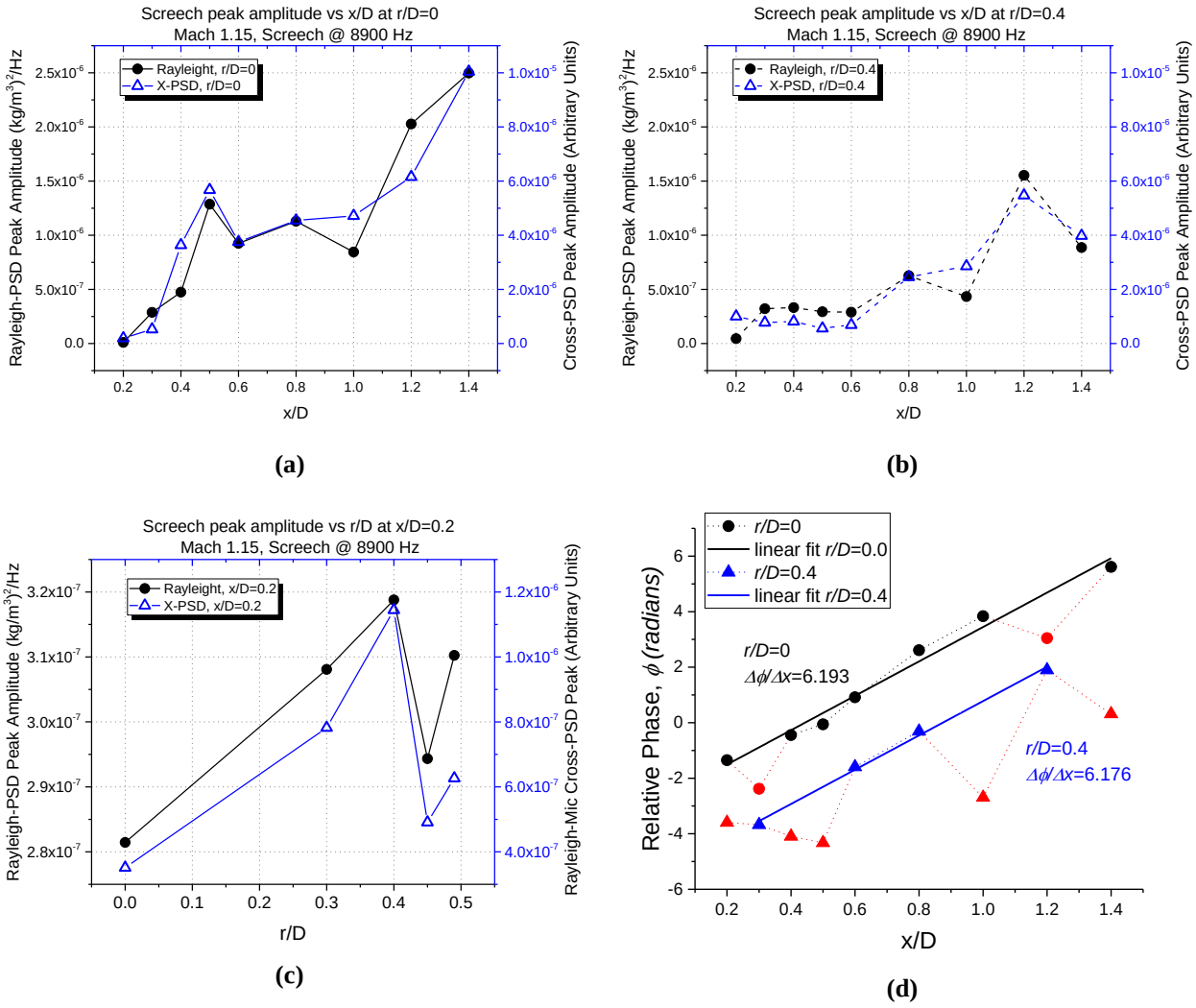

Figure 10. Rayleigh PSD and Rayleigh-Microphone cross-PSD amplitudes at the screech frequency for M_j = 1.15 as a function of (a) *x/D* along the jet centerline, (b) *x/D* along along the jet shear layer (*r/D*=0.4), and (c) *r/D* at an axial station of *x/D*=0.2; (d) Relative cross-spectral phase at the screech frequency as a function of *x/D* along the centerline (*r/D*=0) and the shear layer (*r/D*=0.4).

V. Conclusion

The recently reported 'trapped waves' phenomenon was studied with simultaneous Rayleigh scattering and microphone measurements. The pressure fluctuations associated with these trapped waves were observed as a series of peaks in the SPL spectra from a microphone placed near the edge of the jet and within one jet diameter. Microphone measurements in two different facilities with the same nozzle demonstrated that the phenomenon was a characteristic of the jet flow itself and was not facility dependent. In the present work, gas density fluctuations in a flow issuing from a 1-inch diameter convergent nozzle were measured with a time-resolved, non-invasive, molecular Rayleigh scattering diagnostic while SPL fluctuations were measured simultaneously by a ¼" microphone close to the nozzle exit but outside the flow. The cross-spectra of the two measurements were calculated over a range of separation distances and showed evidence that the trapped wave signature was picked up by the Rayleigh measurements even when not obvious in the Rayleigh measurements themselves. The magnitude of the cross-spectral peaks at the trapped wave frequencies were used to study the modal characteristics of these waves in a high

subsonic flow (M_j = 0.97). An under-expanded flow (M_j = 1.15) with a screech tone at 8900 Hz was also studied. The magnitude and phase of the cross-PSD at the screech frequency were presented. The relative phase as a function of downstream distance provided a measure of the convective Mach number. The current Rayleigh measurements have sufficient SNR to detect Kelvin-Helmholtz waves downstream in the jet and the highest amplitude peak of the trapped waves; however, the SNR needs to be increased for future, more extensive studies of the relatively weak 'trapped waves' via density fluctuation measurements within the jet potential core. The SNR of the Rayleigh measurements will be improved in future experiments by replacing the PMT with a photon detector that has higher sensitivity and lower noise than the current model. In addition, combining increased laser power and direct signal detection at the focus of the collection optics (increasing the signal strength) with much longer time acquisition records (lower the spectral noise floor) will be another method to increase the SNR.

Acknowledgments

The authors thank Ms. Kristie Elam for developing the data acquisition programs and providing acquisition support during the experiments, and Dr. Puja Upadhyay for help in various forms throughout the study. Thanks are also due to Dr. Aaron Towne for inspiring the present experimental effort and for related technical discussions. This work was supported by NASA's Commercial Supersonic Technology (CST) and Transformational Tools & Technologies (TTT) Projects under the Aeronautics Research Mission Directorate (ARMD).

References

[1] Towne, A., Cavalieri, V. G., Jordan, P., Colonius, T., Schmidt, O., Jaunet, V., and Brès, G. A., "Acoustic resonance in the potential core of subsonic jets," *J. Fluid Mechanics*, Vol. 825, 2017, pp. 1113-1152. doi: 10.1017/jfm.2017.346

[2] Suzuki, T., and Colonius, T., "Instability waves in a subsonic round jet detected using a near-field phased microphone array," *J. Fluid Mechanics*, Vol. 565, 2006, pp. 197-226. doi: 10.1017/S0022112006001613

[3] Zaman, K. B. M. Q., and Fagan, A. F., "Near-exit pressure fluctuations in jets from circular and rectangular nozzles," NASA TM-2019-220383, 2019.

[4] Panda, J., and Seasholtz, R. G., "Experimental investigation of density fluctuations in high-speed jets and correlation with generated noise," *J. Fluid Mechanics*, Vol. 450, 2002, pp. 97-130. doi: 10.1017/S002211200100622X

[5] Panda, J., "Two Point Space-Time Correlation of Density Fluctuations Measured in High Velocity Free Jets," AIAA Paper 2006-0006, January 2006. doi: 10.2514/6.2006-6

[6] Zaman, K. B. M. Q., and Fagan, A. F., "Pressure fluctuations due to 'trapped waves' in the initial region of high-speed jets," AIAA Paper 2020-####, AIAA AVIATION Forum, Reno, NV, June 2020.

[7] Welch, P. D., "The use of fast Fourier transform for the estimation of power spectra: a method based on time averaging over short, modified periodograms, *IEEE Trans Audio Electroacoust AU*, Vol. 15, 1967, pp. 70-73. doi: 10.1109/TAU.1967.1161901

[8] Zaman, K. B. M. Q., and Hussain, A. K. M. F., "Natural large-scale structures in the axisymmetric mixing layer," *J. Fluid Mechanics*, Vol. 138, 1984, pp. 325-351. doi: 10.1017/S0022112084000148

[9] Panda, J., Seasholtz, R. G., and Elam, K. A., "Investigation of noise sources in high-speed jets via correlation measurements," *J. Fluid Mechanics*, Vol. 537, 2005, pp. 349-385. doi: 10.1017/S0022112005005148

[10] Panda, J., "An experimental investigation of screech noise generation," *J. Fluid Mechanics*, Vol. 378, 1999, pp. 71-96. doi: 10.1017/S0022112098003383